Article citation info:
Lageweg S, Kubica G. Comparison of traction properties of an N3 category vehicle with a conventional and electric drivetrain. Combustion Engines. 0000;XXX(X):xx-xx. https://doi.org/10.19206/CE-208514

Stefan LAGEWEG
Grzegorz KUBICA

Combustion Engines
Polish Scientific Society of Combustion Engines

Comparison of traction properties of an N3 category vehicle with a conventional and electric drivetrain

ARTICLE INFO

Received: 25 November 2024
Revised: 23 May 2025
Accepted: 22 July 2025
Available online: 27 August 2025

The article presents the traction properties of the drive systems installed in a DAF LF vehicle belonging to the N3 category. Based on technical data of the drive systems – both the compression ignition engine (CI) and electric motor specifications – external characteristics containing the power and torque curves of the engines were developed. On their basis, the traction characteristics of the vehicles were determined, showing graphs of movement resistance and driving force. Graphs of the obtained accelerations, dynamic indicators, and vehicle acceleration simulations were also developed. The calculations considered the case in which the vehicle weight corresponds to the gross vehicle mass (GVM), which allowed for obtaining results close to real conditions.
Based on the comparison of the traction properties of both vehicles, it was observed that electric vehicles have much better dynamic parameters. These differences may be very important when moving in mountain conditions. The excessive propelling force in the system generated by the electric motor allows overcoming hills at a much higher speed, reducing the speed difference between trucks and passenger vehicles. It was found that increasing speed on mountainous roads can lead to significant road safety improvements. The simulation of vehicle acceleration allowed for the determination of the time after which the maximum vehicle speed was achieved.

Key words: *heavy-duty, electric, characteristics, traction, acceleration*

1. Introduction

The continuous development of drivetrain systems contributes to the improvement of the driving characteristics of vehicles. This is especially noticeable in heavy-duty vehicles. This type of vehicle is characterized by a high torque demand in connection with carrying heavy loads [1]. An important aspect occurring while configuring trucks is their drive system, which can differ a lot depending on the purpose of the vehicle [24]. Changes in the configuration of the propelling system have an influence on the traction properties as well as on the energy consumption [12, 21].

Thanks to constant developments of energy storage technology using battery cells and technologies based on the use of energy stored in the form of hydrogen, the range of electric trucks has noticed a marked increase compared to vehicles introduced to the market in the previous decade. Vehicles using energy stored in batteries are nowadays capable of covering an operational range of 400–500 km without the need to recharge their energy reserves. The development of cell production technology has also made it possible to increase their ability to fast charge and superfast charge [5, 22, 23]. Currently produced battery cells are characterized by much higher energy density values and lower initial costs [5, 7].

In the past, battery charging was a very problematic issue, especially for heavy-duty vehicles. The infrastructure did not enable trouble-free operation of electric vehicles due to the insufficient number of charging points or network problems during charging related to exceeding peak network power values. High-power stations designed for fast charging using direct current were one of the causes of network disruptions. Thanks to the introduction of charging stations equipped with BESS technology (battery energy storage system), it is possible to reduce the demand for peak power in the electrical network [2, 14, 17].

Due to the fact that the limitations related to the range and lack of charging possibilities or the duration of the process are becoming much less oppressive, the use of vehicles with an electric drive system is being increasingly considered [20].

This is confirmed by the fact that the number of registrations of delivery vehicles and trucks increased by 66% in the period January–December 2023 compared to the same period in 2022 [10]. It is also worth mentioning the significant development that has been made in terms of the efficiency and flexibility of combustion engines and the significant reduction in exhaust emissions. Modern CI heavy-duty (HV) engines stand out due to the wide range in which the maximum torque is achieved. These are often rotational speeds slightly higher than the idle speed. Work related to the development of combustion engines also focuses on developing new alternative fuels and methods of obtaining them [3, 13, 18, 19].

Despite many advantages modern CI combustion engines offer, these are still not able to match the parameters of electric motors made using permanent magnet synchronous motors (PMSM) technology, with which HDVs are mainly fitted. The configuration of the gearbox drive systems (number of gear ratios, their values), and the value of the final drive ratio make these vehicles stand out with above-average traction properties [11].

The article focuses on the comparison of traction characteristics, allowing to determine, among others, the ability to overcome hills and the time it takes for the vehicle to reach maximum speed. For this purpose, an example vehicle belonging to the N3 vehicle category was taken into account – a representative of the urban and local distribution sector – the field in which electric trucks are currently most commonly used.

2. Research object

The test object is an HDV belonging to the N3 category with a total permissible weight exceeding 19 tons. The DAF LF vehicle (Fig. 1) was first offered with a conventional propulsion system and from 2021 to 2023 with an electric driveline. The truck had been sold as a chassis intended for further body build development. The container built on the vehicle frame was recreated using a computer design program – a CAD program. The installation height and external dimensions were determined based on photo documentation and engineering graphics provided by the chassis manufacturer. Vehicle versions equipped with combustion engines can develop different power and torque values, depending on specifications. For comparison purposes, the variant with the most powerful PX-7 series engine was considered. This engine stands out due to its high torque available in a wide range of rotational speeds. A conventional vehicle has been equipped standardly with a six-speed gearbox with a manual shifting mechanism.

Fig. 1. DAF LF Electric [6]

The electric vehicle (EV) is powered by the SUMO HD HV3500 electric motor and has no gearbox. The vehicle's engine is connected directly via a cardan shaft to the drive axle equipped with a final drive.

Detailed technical data of the vehicle are presented in Table 1.

Table 1. Basic technical data of the researched vehicles

	DAF LF	DAF LF Electric
Engine	PX-7	SUMO HD HV3500
Maximum power [kW]	172	370
Rotational speed of max power [rpm]	2000–2300	3400
Maximum torque [Nm]	900	3445
Rotational speed of max torque [rpm]	1000–1700	150–1050
Main gear ratio	5.13	5.57
Number of gears	6	–
1st gear ratio	6.75	–
2nd gear ratio	3.6	–
3rd gear ratio	2.13	–
4th gear ratio	1.39	–
5th gear ratio	1	–
6th gear ratio	0.78	–
Tire size	R22.5 315/70	
Payload [kg]	11,310	11,700
GVM [kg]	19,000	

According to the information provided by the vehicle manufacturer, both versions of the vehicle have a GVM of exactly 19 tons. The aerodynamic properties of the vehicles are the same.

This selection of the research facility allowed for the elimination of variables unrelated to the drive system itself.

3. Methodology

To prepare the traction characteristics of the vehicle, it was necessary to determine the external characteristics of the engines. For this purpose, technical data provided by the vehicle manufacturer and manufacturers of drive system components were used.

Determining the operating characteristics of the electric motor required reproducing the torque waveform, and, on this basis, the engine power was determined. That enabled the creation of the power and torque charts for both engines. The comparison of the vehicle's traction characteristics consisted of determining the external characteristics of the engines and the vehicle's movement resistance.

In the following, the forces acting on the vehicle during its movement were determined. Due to the small impact of some resistances, they were not taken into account in the calculations. The most important resistances to the movement of vehicles were taken into account. In the research, the following forces were taken into consideration:

– rolling resistance
– aerodynamic resistance
– hill resistance.

The calculated aerodynamic drag forces can differ from the real forces as a result of the needed assumptions. Due to the lack of a defined air resistance coefficient in the longitudinal direction from the vehicle axis (C_x factor), it was necessary to determine the value used in the calculations. The value was selected based on the table [4] and on the author's knowledge about the development of aerodynamic properties in trucks and buses.

The frontal surface area for the vehicle under consideration was determined by plotting the outline of the body on the cabin design. The contours of the vehicle's front obtained in this way were printed on graph paper, and its area was calculated.

In the calculations, in order to make the results more realistic, the vehicle weight value resulting from the maximum permissible total vehicle weight was assumed.

As part of the study, a simulation of vehicle acceleration was also carried out in the speed range from 0 km/h to 90 km/h. It was decided to set a maximum speed equal to the speed at which the vehicles can move due to the electronic speed limiter, which is obligatory for every HDV. The simulation is based on the use of maximum instantaneous accelerations and a simple algorithm that allows for the simulation of gear changes. When the previously defined maximum engine speed is reached, a gear change takes place, which lasts a certain time; in the case of a manual gearbox, this time is set at 1.5 seconds [14]. The gear change time is understood as the time from the moment of disengaging the clutch to the moment of engaging it after the next gear is selected.

4. Engine characteristics

4.1. Paccar PX-7

In the case of the Paccar PX-7 engine, creating a graph of the engine's external characteristics involved reflecting the power and torque curves. In this case, the manufacturer provided full external characteristics of the engine. The developed power and torque values are presented in Table 2. The characteristic curve is shown in Fig. 2.

Table 2. Power and torque values for the propulsion engines

n [rpm]	Power [kW]		Torque [Nm]	
	SUMO HD HV3500	PX-7	SUMO HD HV3500	PX-7
0	0	–	2800	–
100	34	–	3230	–
200	72	–	3445	–
300	108	–	3445	–
400	144	–	3445	–
500	180	–	3445	–
600	216	–	3445	–
700	252	–	3445	–
800	288	–	3445	–
900	325	–	3445	–
1000	361	94	3445	900
1100	370	104	3214	900
1200	370	113	2946	900
1300	370	122	2719	900
1400	370	132	2525	900
1500	370	141	2357	900
1600	370	151	2209	900
1700	370	160	2079	900
1800	370	165	1964	874
1900	370	169	1861	848
2000	370	172	1768	822
2100	370	172	1683	783
2200	370	172	1607	747
2300	370	172	1537	714
2400	370	163	1473	650
2500	370	153	1414	586
2600	370	–	1360	–
2700	370	–	1309	–
2800	370	–	1263	–
2900	370	–	1219	–
3000	370	–	1178	–
3100	370	–	1140	–
3200	370	–	1105	–
3300	370	–	1071	–
3400	370	–	1040	–

4.2. Sumo HD HV3500

On the basis of catalogue data, engine calibration instructions, and the torque curve (Fig. 2), the external operating characteristics of the electric motor were determined. For this purpose, the following patterns were used:

For the rotational speed range of 0–1000 rpm, the power was determined using the power dependence on the torque and engine speed (1). Torque for rotational speeds 1026–3400 rpm had been determined by using the same formula.

$$P = \frac{T\,[Nm] \cdot n[rpm]}{9554.14}\,[kW] \tag{1}$$

where: P – power, T – torque, n – rotational engine speed

In order to recreate the linear torque waveform in the rotational speed range from 0 till 1026 rpm, the directional equation of a straight line passing through two points (equation 2) plotted on the torque waveform was used (Fig. 2).

Points coordinates:

- A (0 rpm; 2800 Nm)
- B (150 rpm; 3445 Nm).

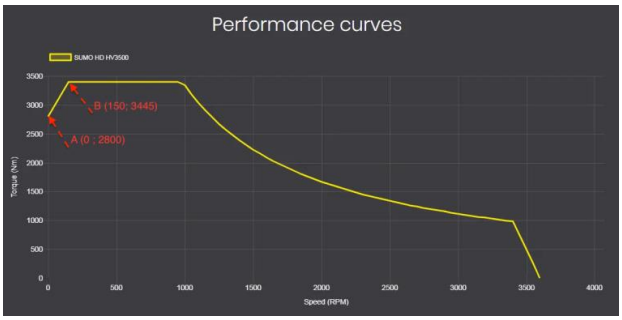

Fig. 2. Torque curve of the SUMO HD HV3500 engine [1]

$$y - y_A = \frac{y_B - y_A}{x_B - x_A} \cdot (x - x_A) \tag{2}$$

where: XA, Y_A – coordinates of point A, X_B, Y_B – coordinates of point B.

The calculated power and torque values depending on the engine speed are presented in Table 2. The operating characteristic curve of the drive unit is shown in Fig. 3.

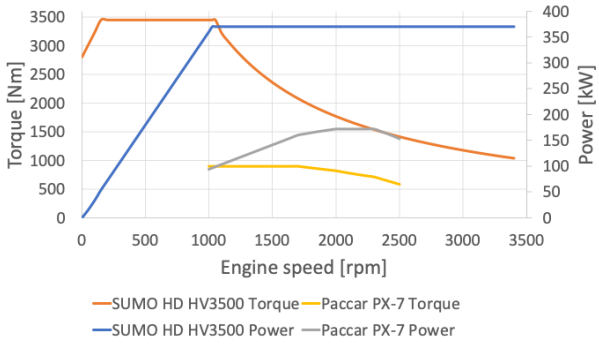

Fig. 3. Engine characteristics

5. Forces acting on the vehicle

Both versions of the vehicle – conventional and electric are characterized by identical movement resistance, which results from the previously made assumptions and technical data of the bodywork. Identical values were maintained for all coefficients during the calculation.

Due to the small share of specific types of resistance in the total resistance force of all vehicle movement resistances acting on it, it was decided to ignore their influence. Forces not included in the simulation include resistances such as:

- resistance of wet surface
- friction resistance of bearings
- resistances related to the tires and resulting from the operation of the suspension and steering system, i.e. wheel turning resistance, toe-in resistance, tire deformation
- resistance resulting from turning – driving in a straight direction was assumed.

Rolling resistance

In the case of HDVs, rolling resistance has a much greater impact on the vehicle's energy consumption than in the case of passenger vehicles, which results directly from

the large weight of the vehicles. The rolling resistance (3) coefficient f_t depends, among other things, on the square of the vehicle's speed and the surface resistance coefficient. For the calculations, an approximate value corresponding to dry asphalt $f_0 = 0.01$ was assumed. To calculate the force the formula (3) was used.

$$F_t = G \cdot f_t = mgf_o(1 + kv^2)\ [N] \tag{3}$$

where: G – vehicle weight, f_t – rolling resistance coefficient, m – mass, g – acceleration of gravity, f_0 – surface rolling resistance coefficient, k – surface coefficient, v – speed.

5.1. Aerodynamic forces

Due to the assumptions made, the simplified formula was used to calculate aerodynamic resistance. The formula uses a conversion factor of 0.047, which replaces the speed converter, allowing the use of speed expressed in kilometres per hour instead of meters per second, and is the result of using the average air density. The formula (4) was used to calculate the aerodynamic drag force.

$$F_a = 0.047 \cdot A \cdot c_x \cdot v^2\ [N] \tag{4}$$

where: Fa – aerodynamic resistance force, A – frontal vehicle surface, c_x – aerodynamic coefficient, v – speed.

The approximate frontal area of the vehicle assumed in the calculations was determined of 8.59 m^2 [9].

5.2. Hill resistance force

The hill's resistant forces are a major obstacle for HDVs when trying to maintain a constant speed or accelerate. The significant weight of the vehicle means that even small slopes can generate very high resistance values, which the vehicle must additionally overcome. In many cases, a significant difference in the vehicle's speed is observed when entering a slope.

The values of the slope angle of driveways are regulated by law and depend on the class the road fulfills and its function. In case of local and access roads with a maximum speed of 30 km/h or 40 km/h, the gradient can be up to 12%. However, heavy goods vehicles mostly travel on highways and urban roads. The permissible slope angle of two-lane roads in the city area is in the range of 4–5% [16].

In order to determine the slope resistance value, a slope of 4% was assumed, and the equation underneath (5) was used.

$$F_w = G \cdot \frac{h_w}{100\%}\ [N] \tag{5}$$

where: F_w – hill resistance force, G – vehicle weight, h_w – slope.

5.3. Propelling force

The formula (6) was used to calculate the driving force in the drive system. The calculations required the assumption that the efficiency of the drive system was 0.9. During the calculations of driving forces for the electric vehicle that was not equipped with a gearbox, the gear ratio was omitted from the calculations

$$F_n = \frac{T \cdot i_{SB} \cdot i_o \cdot \eta_m}{r_d}\ [N] \tag{6}$$

where: F_n – propelling force, T – torque, i_{SB} – gear ratio, i_o – main gear ratio, η_m – mechanical efficiency, r_d – dynamic radius of rolling tyre.

5.4. Vehicle speed

Determining the vehicle speed for each gear was necessary to create graphs of driving force, dynamic index and acceleration. These values change depending on the instantaneous speeds (7) at which the vehicle is moving.

$$v = 0.377 \frac{r_d \cdot n}{i_{sb} \cdot i_o}\ [\frac{km}{h}] \tag{7}$$

where: v – speed, r_d – dynamic radius of rolling tyre, n – rotational engine speed [rpm], i_{SB} – gear ratio, i_0 – main gear ratio.

5.5. Vehicle acceleration

Calculating the vehicle acceleration (8) allowed to determine the maximum acceleration values the vehicle can achieve in a given gear and at given driving speeds. This value depends on the value of the vehicle dynamic index and rotating masses for a given gear. These two values will mainly determine the increase in acceleration.

$$a = \frac{(D - f_t) \cdot g}{\delta}\ [\frac{m}{s^2}] \tag{8}$$

where: a – acceleration, D – dynamic index, f_t – rolling resistance coefficient, g – acceleration of gravity, δ – rotating mass coefficient.

5.6. The condition of maintaining adhesion

The condition of maintaining adhesion is particularly important from the point of view of vehicle movement safety. It expresses the maximum value of the driving force on the vehicle wheels, at which wheel slippage does not occur. The condition is expressed by the equation (9).

$$F_n = F_p \tag{9}$$

$$\frac{M_r \cdot i_{SB} \cdot i_0 \cdot \eta_m}{r_d} = G_T \cdot m_t \cdot \mu \tag{10}$$

where: F_n – propelling force, F_p – Wheel adhesion force, M_r – Torque used by setting the vehicle into motion, i_{SB} – gear ratio, i_0 – main gear ratio, η_m – mechanical efficiency, r_d – dynamic radius of rolling tire, G_T – drive axle load, m_t – mass displacement factor, μ – rolling resistance coefficient for dry asphalt.

The maximum engine torque that can be used to start the vehicle without losing traction of the drive wheels on a dry asphalt surface was determined based on equation (10). The maximum torque is determined by formula (11). The drive axle load was assumed to be 11.5 tons. The displacement coefficient m_t was assumed to be 1.15, and the gear ratio values for both vehicles were used. The results for the first three gears are presented in table 3.

$$M_r = \frac{G_T \cdot m_t \cdot \mu \cdot r_d}{i_{SB} \cdot i_0 \cdot \eta_m} \tag{11}$$

where: M_r – torque used by setting the vehicle into motion, G_T – drive axle load, m_t – mass displacement factor, μ – rolling resistance coefficient for dry asphalt, r_d – dynamic radius of rolling tire, i_{SB} – gear ratio, i_0 – main gear ratio, η_m – mechanical efficiency.

The maximum torque values that can be used when starting vehicles with no risk of skid are higher than the maximum torque values generated by vehicle engines. There is no risk of wheel slippage during acceleration using the maximum torque on a dry asphalt surface.

Table 3. Adhesion force of the drive axle and the maximum torque values for each gear of the vehicles

	DAF LF Electric	DAF LF
Gt [N]	112815.0	112815.0
Fp [N]	116763.5	116763.5
Mr (i_1) [Nm]	11319.9	1820.8
Mr (i_2) [Nm]	–	3414.1
Mr (i_3) [Nm]	–	5770.3

Using equation (12), the maximum values of the gear ratios of the gearbox had been determined. Depending on the torque used to bring the vehicle into motion, the ratio value changes. The results are presented in Table 4.

$$i_{SB} = \frac{G_T \cdot m_t \cdot \mu \cdot r_d}{M_r \cdot i_0 \cdot \eta_m} \quad (12)$$

where: G_T – drive axle load, m_t – mass displacement factor, μ – rolling resistance coefficient for dry asphalt, r_d – dynamic radius of rolling tire, M_r – torque used by setting the vehicle into motion, i_0 – main gear ratio, η_m – mechanical efficiency.

Table 4. Calculated ratio values depend of the torque used by setting the vehicle into motion

DAF LF Electric		DAF LF	
M_r [Nm]	i_{SB}	M_r [Nm]	i_{SB}
900	12.6	400	30.7
1300	8.7	500	24.6
1700	6.7	600	20.5
2100	5.4	700	17.6
2500	4.5	800	15.4
2900	3.9	900	13.7
3300	3.4	–	–
3500	3.23	–	–

The i_{SB} ratios presented in Table 4 are the maximum values, depending on the starting torque, at which traction of the drive wheels is maintained. All the ratios determined are greater than those available to both vehicles.

6. Discussion of results

6.1. Introduction

The calculated values of the resistance forces were approximated to decimal digits. Due to the lack of knowledge of the maximum design speed of the vehicles, calculations were made for speeds up to 120 km/h. In EU member states, heavy goods vehicles must be equipped with an electronic speed limiter limiting the speed to a maximum of 90 km/h. However, the manufacturer could have provided a different maximum speed for the vehicle in order to create excess driving force.

In order to maintain the accuracy of the calculations, they were carried out starting from a speed of 0 km/h and increasing it by 1 km/h until the speed of 120 km/h was reached.

The forces of resistance and the driving force of the vehicles are presented in the graph in Fig. 4. It shows the values of the driving force for both drive systems.

6.2. Acceleration ability

The driving and resistance force graph (Fig. 4) shows the change in driving force for each gear and movement resistances for vehicles as a function of vehicle speed.

Analyzing the graph, it can be seen that the driving force curve for an electric vehicle is characterized by a lower maximum value of the driving force in comparison with the first gear. In addition to a combustion engine vehicle, it is continuous and flattened in the speed range from 5 km/h to about 40 km/h.

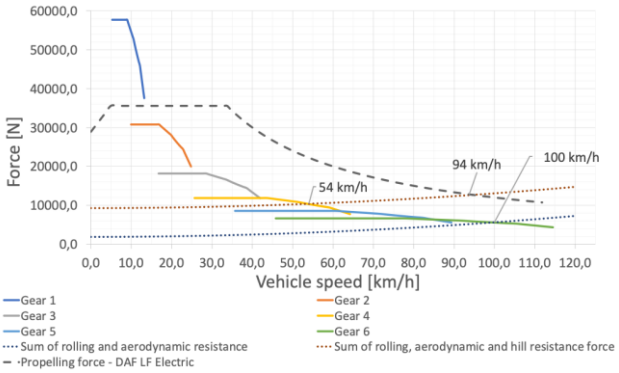

Fig. 4. Forces acting on the vehicles

The continuity of the driving torque is caused by the lack of a gearbox and the ability to reach high rpm values by the electric motor.

This enables accelerating without momentarily losing the driving force on the vehicle's wheels. It is crucial not to lose momentum when overcoming steep slopes. A gear change causes a lack of driving force. In extreme cases, this may cause the vehicle to stop and then roll down the slope or damage components such as the clutch by overheating it while trying to move the vehicle from a still stand. A vehicle powered by a drive system based on an electric motor allows for continuous acceleration without fear of losing driving torque.

The excess driving force of the electric vehicle allows it to overcome a 4% gradient at a maximum speed of 94 km/h. Knowing that the vehicle must be equipped with a system limiting the maximum speed to 90 km/h, it can be stated that the vehicle is capable of overcoming hills with the same or slightly bigger slopes without losing speed while driving at maximum speed. The DAF LF is capable of overcoming the same gradient at a maximum speed of around 54 km/h and requires shifting down from sixth to the fourth gear. This causes significant inconvenience in driving the vehicle because overcoming a four percent gradient with a conventional vehicle requires much more attention from the driver and is less economical due to the change in driving speed and the need to accelerate again after overcoming the hill. Losing speed by 36 km/h can also lead to dangerous situations, e.g., when driving on a motorway. The difference in speed of vehicles moving on a gradient on expressways can be even 86 km/h in this case. A passenger car hitting the back of a truck is comparable to a collision with a stationary obstacle at a speed resulting from the speed difference between the vehicles. The dynamic characteristics graph (Fig. 5) for the vehicles illustrates the excess driving force. Comparing both drive systems, it can be noticed that the conventional drive is characterized by a driving force surplus greater than the electric system only in first gear. The electric vehicle is character-

ized by a generally greater driving force surplus at speeds higher than the minimum driving speed in the second gear for the traditional drive.

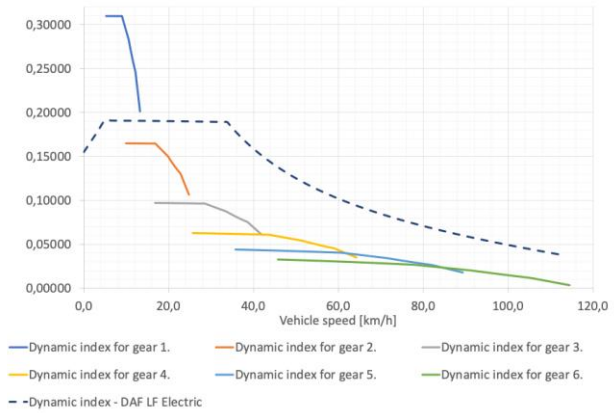

Fig. 5. Dynamic indexes for the vehicles

Comparing the dynamic index graph (Fig. 5) with the acceleration graph (Fig. 6), it can be seen that the acceleration values for the second gear in the DAF LF are higher than for the first gear. This is due to the much higher value of the rotating mass coefficient for the first two gears, which are $\delta_1 = 4.19$ and $\delta_2 = 1.9$. The lower mass of the rotating elements in the drive system and gearbox affects the vehicle acceleration values and its energy consumption [23].

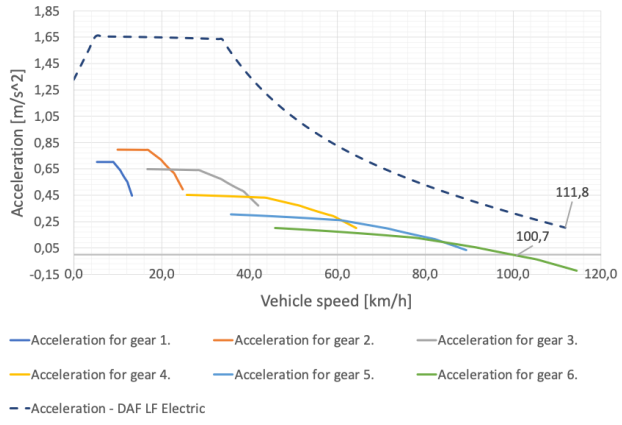

Fig. 6. Vehicle accelerations

The small number of rotating elements in the electric vehicle drive contributes to the improvement of the dynamic qualities of this vehicle. Analyzing the above placed graphs, it can also be seen that the truck is capable of reaching a higher maximum speed, which is approximately 110 km/h, only due to reaching the maximum rpm of the electric engine. Higher maximum speeds that these vehicles are able to reach may result in an increase in the speed limit for trucks in the future, if, together with the capabilities of the drive system, the braking system, and suspension are improved. Increasing the maximum speed at which trucks can move may result in improved safety as a result of the reduced speed difference between vehicles. To precisely determine the effects of changing the speed limit for trucks, research should be carried out by road safety specialists. Currently, these statements are only assumptions.

The simulation of vehicle acceleration was made for the speed range of 0–90 km/h. Figure 7 shows how the speed of the vehicles changed over time. It can be seen that the need to change gears increased the time needed to reach the speed limited by the electronic speed limiter. During the gear change in the vehicle, no torque is supplied. This causes the vehicle to move with a negative acceleration value due to the resistance of movement; as a result, its speed decreases. The simulation was carried out for an even surface. The simulation shows that the electric vehicle is able to reach 90km/h in just 26 seconds, while the conventional HDV needs 83 seconds more.

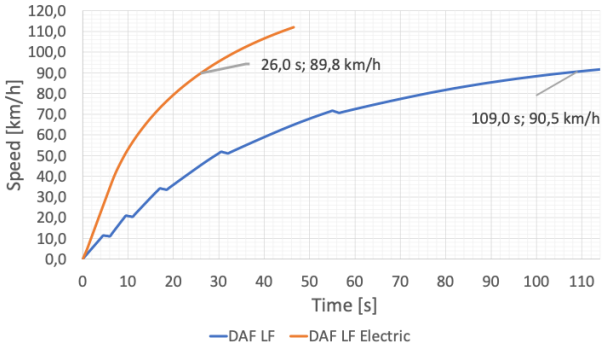

Fig. 7. Acceleration simulation

The time it takes for the vehicle to reach a given speed is important because it will affect the fluidity of vehicle traffic, especially in urban areas where many intersections are placed. This will lead to an increase in the number of vehicles passing intersections. Similarly to the overall higher speed of driving on an incline by an electric vehicle, reaching a given speed faster can contribute to road safety improvements. Currently, it can be very often noticed that passenger cars starting at an intersection firstly accelerate more than they can and then decelerate due to the slower HDV in front of them. That phenomenon results in a wave effect, which in radical conditions can lead to a complete stop of the vehicles far behind the truck. It is possible that with the participation of electric vehicles, this phenomenon will disappear due to the reduction of the difference in acceleration between passenger cars and trucks.

6.3. Speeds at slopes

When analyzing the maximum speeds of climbing hillsides with different degrees of inclination, it can be seen that a vehicle equipped with an electric drive is able to overcome them at higher speeds (Fig. 8) however, it should be noted that the maximum possible slope on which the vehicle can drive equals 18%, while for a vehicle with a conventional drive system it is 30%. The largest speed difference between the vehicles is 41.4 km/h for a hillside of 4%, and the smallest for 18% and equals 6.8 km/h.

The speed curve of overcoming slopes with increasing inclination in the case of a vehicle with a traditional drive system takes the form of an exponentially decreasing function. In the case of a vehicle with an electric drive, the speed in the initial phase decreases proportionally to the value of about 10% of the grade. Then the line of the maximum speed of overcoming hills becomes gentler, and be-

tween the slope value of 16% and the maximum, it drops significantly.

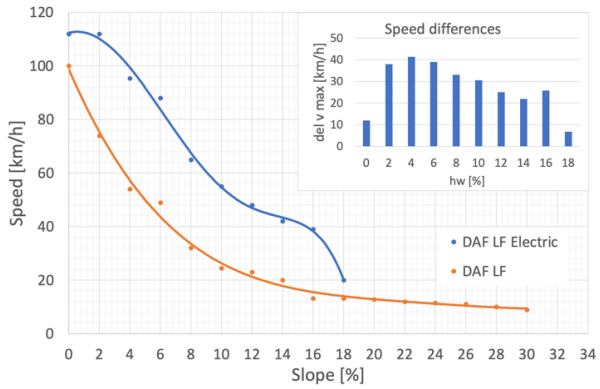

Fig. 8. Vehicle speed and the differences between their maximum values

In connection with the above advantages of electric drives, it can be assumed that in the future, further development of manufacturing techniques will enable the construction of lighter vehicle structures. Changes to Regulation 96/53/EC consist of changes to Article 9a related to the maximum vehicle length, allowing registration of 90cm longer vehicles after 1 September 2020, under the condition that this does not increase the vehicle's load capacity, and these changes will improve the aerodynamic properties and safety of the vehicle. With the development of electromobility and the popularization of electric heavy goods vehicles, proposals have appeared to introduce changes to the regulations that would allow for an increase in the permissible total masses for electric vehicles by four tons. The above study of the traction properties of an electric vehicle confirms the validity of the desire to introduce changes. However, it is necessary to bear in mind issues related to decelerating and bringing to a stillstand vehicles with a greater mass. Simulation studies should be carried out and verified in real conditions in order to determine to what extent an increase in vehicle mass by four tons will affect the vehicle's braking distance, which directly relates to road safety.

7. Conclusions

The traction properties of the drive system of a vehicle equipped with an electric motor causes a significant improvement in vehicle movement properties thanks to the use of these engines for propulsion. The different properties of electric vehicles compared to combustion-powered vehicles suggest that these vehicles may be used in specific conditions. The use of electric motors to support the drive by creating a hybrid vehicle is a good solution to improve the vehicle's traction properties and maintain a large operational range of the vehicle. In addition, the following conclusions can be specified:

1. The maximum acceleration of an electric vehicle is double the maximum of a vehicle with a conventional drivetrain. No need for gear changes increases the acceleration ability and makes it continuous – not interrupted.
2. The electric vehicle characterizes a short time needed to reach the maximum speed (26 seconds), which is possible due to high acceleration values and continuous drive torque.
3. A conventional vehicle can drive on slopes up to 30% while the electric vehicle has the ability to overcome hills up to 18%, but it drives on them at higher speeds.
4. The biggest difference in speed while driving on terrain elevations is 41.4 km/h for a 4% slope.
5. Higher speeds while overcoming slopes by the electric vehicle can cause a smaller risk of rear-end collisions with cars.
6. Carrying out research in the field of road safety is essential to determine the influence of electric trucks and their traction properties on safety, and to determine the ability of increasing speed limits and GVM by 4 tons.

To reach a higher speed on slopes, a very high torque is needed. Using the highest torque of the engine for a long time can cause a rapid increase in energy consumption and affect the maximum 280 km operational range. Due to the ability of regenerative braking, it is possible to partly reduce the declining rate of the vehicle range depending on the mass of the truck [6].

Nomenclature

a	acceleration
A	frontal vehicle surface
BESS	battery energy storage system
CAD	computer aided design
CI	compression ignition
C_x	aerodynamic coefficient
D	dynamic index
EV	electric vehicle
f_0	surface rolling resistance coefficient
f_t	rolling resistance coefficient
F_a	aerodynamic resistance force
F_n	propelling force
F_t	rolling resistance force
F_w	hill resistance force
g	acceleration of gravity
G	vehicle weight
GVM	gross vehicle mass
h_w	slope
HV	heavy-duty
HDV	heavy-duty vehicle
i_0	main gear ratio
i_{SB}	gear ratio
k	surface coefficient
m	mass
n	rotational engine speed [rpm]
P	power [kW]
PMSM	permanent magnet synchronous motor
r_d	dynamic radius of rolling tyre
T	torque [Nm]
v	speed
X_A, Y_A	coordinates of point A
X_B, Y_B	coordinates of point B
δ	rotating mass coefficient
η_m	mechanical efficiency

Bibliography

[1] Bernatchez O. 4 new powertrain options available with increased performances. https://www.danatm4.com/4-new-powertrain-options-available-with-increased-performances/

[2] Bertucci JP, Hofman T, Salazar M. Joint optimization of charging infrastructure placement and operational schedules for a fleet of battery electric trucks. 2024 American Control Conference, ACC 2024. Institute of Electrical and Electronics Engineers. 2024:2995-3000. 10644339 https://doi.org/10.23919/ACC60939.2024.10644339

[3] Bielaczyc P, Woodburn J, Joshi A. World-wide trends in powertrain system development in light of emissions legislation, fuels, lubricants, and test methods. Combustion Engines. 2021;184(1):57-71. https://doi.org/10.19206/CE-134785

[4] Biliński J, Błażejewski M, Malczewska M, Szczepiórkowska M, Drag resistance of electric buses and trolleybuses - empirical formulae. TTS Technika Transportu Szynowego 2020;9:48-52. http://yadda.icm.edu.pl/baztech/element/bwmeta1.element.baztech-28e29698-6f1e-4c3f-8bf1-9943f41aceb7/c/BilinskiTTS9.pdf

[5] Campillo J, Dahlquist E, Danilov DL, Ghaviha N, Notten PHL, Zimmerman N. Battery technologies for transportation applications. in: technologies and applications for smart charging of electric and plug-in hybrid vehicles. Springer International Publishing. Cham 2017:151-206. https://doi.org/10.1007/978-3-319-43651-7_5

[6] DAF LF Electric — pojazd ciężarowy o zerowym poziomie emisji spalin przeznaczony do dystrybucji miejskiej. DAF Trucks Polska SP. z o. o. https://www.daftrucks.pl/pl-pl/wiadomosci-oraz-media/news-articles/global/2021/q1/27-01-2021-daf-lf-electric-for-zero-emission-urban-distribution

[7] Hemlecki P, Fabiś P. Formula Student class electric vehicle energy storage – study and design assumptions. Combustion Engines. 2024;198(3):54-61. https://doi.org/10.19206/CE-186164

[8] Karakas O, Seker U, Solmaz H. Modeling of an electric bus using MATLAB/Simulink and determining cost saving for a realistic city bus line driving cycle. Engineering Perspective. 2021;1(2):52-62. https://doi.org/10.29228/eng.pers.51422

[9] Lageweg S. Electric drive development in heavy-duty vehicles and buses [Master's thesis]. Silesian University of Technology. Katowice 2024.

[10] Licznik Elektromobilności: Podsumowanie 2023 r. w sektorze zeroemisyjnego transportu. PSNM – Polskie Stowarzyszenie Nowej Mobilności. 2024. https://psnm.org/2024/informacja/licznik-elektromobilnosci-podsumowanie-2023-r-w-sektorze-zeroemisyjnego-transportu/

[11] Łebkowski A. Electric vehicles trucks – overview of technology and research selected vehicle. Scientific Journal of Gdynia Maritime University. 2017;98:157-166. https://sj.umg.edu.pl/sites/default/files/ZN506.pdf

[12] Mayet C, Welles J, Bouscayrol A, Hofman T, Lemaire-Semail B. Influence of a CVT on the fuel consumption of a parallel medium-duty electric hybrid truck. Math Comput Simulat. 2019;158:120-129. https://doi.org/10.1016/j.matcom.2018.07.002

[13] Orliński P, Sikora M, Bednarski M, Laskowski PP, Gis M, Wiśniowski PK. Evaluation of selected combustion parameters in a compression-ignition engine powered by hydrogenated vegetable oil (HVO). Combustion Engines. 2024; 198(3):34-40. https://doi.org/10.19206/CE-184222

[14] Polat H, Hosseinabadi F, Hasan MM, Chakraborty S, Geury T, El Baghdadi M et al. A review of DC fast chargers with BESS for electric vehicles: topology, battery, reliability oriented control and cooling perspectives. Batteries. 2023;9(2): 121. https://doi.org/10.3390/batteries9020121

[15] Prażnowski K, Drabik D. Analysis of composition of linear acceleration body structure of vehicle during the gear changing. Autobusy – Technika Eksploatacja Systemy Transportowe. 2018;19(6):678-681. http://doi.org/10.24136/atest.2018.155

[16] Rozporządzenie Ministra Transportu i Gospodarki Morskiej z dnia 2 marca 1999 r. w sprawie warunków technicznych, jakim powinny odpowiadać drogi publiczne i ich usytuowanie (in Polish).

[17] Saldanha JJA, Nied A, Trentini R, Kutzner R. AI-based optimal allocation of BESS, EV charging station and DG in distribution network for losses reduction and peak load shaving. Electr Pow Syst Res. 2024;234:110554. http://doi.org/10.1016/j.epsr.2024.110554

[18] Skobiej K. A review of hydrogen combustion and its impact on engine performance and emissions. Combustion Engines. 2025;200(1):64-70. https://doi.org/10.19206/CE-195470

[19] Smolec R, Karpiuk W, Bajerlein M, Waligórski M, Kril P. The use of dimethyl ether (DME) solution in compression ignition engine. Combustion Engines. 2024;198(3):123-128. https://doi.org/10.19206/CE-188832

[20] Verbruggen FJR, Hoekstra A, Hofman T. Evaluation of the state-of-the-art of full-electric medium and heavy-duty trucks. 31st International Electric Vehicle Symposium and Exhibition, EVS 2018 and International Electric Vehicle Technology Conference 2018, EVTeC 2018. B4-5.

[21] Verbruggen FJR, Silvas E, Hofman T. Electric powertrain topology analysis and design for heavy-duty trucks. Energies. 2020;13(10):2434. http://doi.org/10.3390/en13102434

[22] Yamada T, Akisawa A. Effectiveness of high-power chargers at a quick-charging station for electric vehicles. Appl Energ. 2025;377:124623. http://doi.org/10.1016/j.apenergy.2024.124623

[23] Yao C, Chen S, Salazar M, Yang Z. Joint routing and charging problem of electric vehicles with incentive-aware customers considering spatio-temporal charging prices. IEEE T Intell Transp. 2023;24(11):12215-12226. http://doi.org/10.1109/tits.2023.3286952

[24] Zielińska E, Skalski B. Characteristics of traction properties of selected car models. Autobusy: technika, eksploatacja, systemy transportowe. 2016;17(12):1524-1527 http://yadda.icm.edu.pl/baztech/element/bwmeta1.element.baztech-4ce58b40-a854-42b6-b375-32b2d2dce3a8

Stefan Lageweg, MEng. – Faculty of Transport and Aviation Engineering, Silesian University of Technology, Katowice, Poland.
e-mail: *lagewegstefan@gmail.com*

Grzegorz Kubica, DSc., DEng. – Faculty of Transport and Aviation Engineering, Silesian University of Technology, Katowice, Poland.
e-mail: *grzegorz.kubica@polsl.pl*